Available online at www.sciencedirect.com
ScienceDirect
Molecular Immunology 45 (2008) 1221–1230
Molecular Immunology
www.elsevier.com/locate/molimm

Toward an atomistic understanding of the immune synapse: Large-scale molecular dynamics simulation of a membrane-embedded TCR–pMHC–CD4 complex

Shunzhou Wan [a], Darren R. Flower [b], Peter V. Coveney [a,*]

[a] *Centre for Computational Science, Department of Chemistry, University College London, 20 Gordon Street, London WC1H 0AJ, UK*
[b] *The Jenner Institute, University of Oxford, Compton, Berkshire, UK*

Received 23 July 2007; accepted 22 September 2007
Available online 5 November 2007

Abstract

T-cell activation requires interaction of T-cell receptors (TCR) with peptide epitopes bound by major histocompatibility complex (MHC) proteins. This interaction occurs at a special cell–cell junction known as the immune or immunological synapse. Fluorescence microscopy has shown that the interplay among one agonist peptide-MHC (pMHC), one TCR and one CD4 provides the minimum complexity needed to trigger transient calcium signalling. We describe a computational approach to the study of the immune synapse. Using molecular dynamics simulation, we report here on a study of the smallest viable model, a TCR–pMHC–CD4 complex in a membrane environment. The computed structural and thermodynamic properties are in fair agreement with experiment. A number of biomolecules participate in the formation of the immunological synapse. Multi-scale molecular dynamics simulations may be the best opportunity we have to reach a full understanding of this remarkable supra-macromolecular event at a cell–cell junction.

Keywords: Immunological synapse; Molecular dynamics; High performance computing

1. Introduction

The ostensive function of the immune system – defense against pathogens – manifests itself through a remarkable network of cooperating agents exhibiting behaviour on several characteristic length scales. The immune system is dynamic, hierarchical and many levelled, operating at the scale of organs, through tissues, down to cells, molecules, and ions.

Arguably, the most important – and certainly one of the most interesting – length scales within immunology reside at the mesoscale, which comprises supramolecular scenarios ranging in size from 10 to 100 nm. An example of such a phenomenon is the so-called immunological synapse (IS) (Grakoui et al., 1999). Communication between antigen-presenting cell (APC) and T cell occurs at the immunological synapse: a specialized cell–cell junction characterized by its relative stability, sustained signalling, and by an ordered series of complex coordinated events within both cells. The partnership between APCs and T cells helps the body to defend itself against insurgent pathogens of all kinds: viruses, bacteria, eukaryotic parasites, and aberrant host cells. The APC–T cell interface is the site of the recognition of major histocompatibility complex molecule-peptide (pMHC) complexes by T-cell receptors (TCRs), the key molecular event at the heart of the immune response.

The canonical structure of the IS involves formation of an interface between APC and T cell. The IS is no empty lacuna, but is densely populated by signalling and adhesion molecules. Rings composed of talin, together with complexes between leukocyte function-associated antigen 1 (LFA-1) and intercellular adhesion molecule 1 (ICAM-1), form around a central cluster consisting of pMHC–TCR complexes and protein kinase

Abbreviations: IS, immunological synapse; MD, molecular dynamics; TCR, T-cell receptor; MHC, major histocompatibility complex; pMHC, peptide-major histocompatibility complex; pMHCII, peptide-major histocompatibility complex class II; APC, antigen-presenting cell; PDB, protein data bank; RMS, root-mean-square; MM/PBSA, molecular mechanics Poisson–Boltzmann surface area; CG, coarse-grained.

* Corresponding author. Tel.: +44 20 7679 4560; fax: +44 20 7679 1501.
E-mail address: p.v.coveney@ucl.ac.uk (P.V. Coveney).

0161-5890/$ – see front matter © 2007 Elsevier Ltd. All rights reserved.
doi:10.1016/j.molimm.2007.09.022

C-θ. Thus the mature IS, which is characterized by a stable distribution of membrane proteins, consists of two functional domains: a central cluster of TCR–pMHC complexes and a surrounding ring of adhesion molecules. Segregation of adhesion molecules and TCRs is thought to be mediated primarily by size. The pMHC–TCR pair is about 15 nm in length while the LFA-1–ICAM-1 pair is much longer, about ∼42 nm. Two segregated patterns in the junction are favourable because of the lower energetic cost of bending the cell membranes to accommodate two domains separately. The differences in length between these regions create a functionally important supramolecular structure at the mesoscale and beyond. Indeed, the IS can be visualized using light microscopy (Huppa and Davis, 2003).

The structure of the mature IS appears to differ significantly between different cell types. The previously described classical bull's eye pattern formed with B cells, or with supported planar bilayers, exhibits a central focus of interacting TCR–pMHC complexes (Bromley et al., 2001). Dendritic cells, on the other hand, display an IS which has multiple foci of interaction with the T cell (Dustin et al., 2006).

Multiple kinds of experimental study have demonstrated the clustering of TCRs and pMHCs, as well as other specific molecules at the interface. These experiments give us an extensive, yet ultimately incomplete, cellular and molecular view of the IS (Bromley et al., 2001). On the other hand, structural studies of molecules comprising the IS reveal atomistically resolved yet static views of the individual molecular recognition events involved (Wang and Eck, 2003). No experimental method is able to tell us all we want or need to know. No combination of methods, at the molecular level, adequately explains all observations of the IS. We need to escape the constraints of purely experimental study and explore the IS computationally if we are to address these deficiencies in understanding.

As a complete view of the IS is beyond the scope of current experimental protocols, several theoretical methods have been proposed to model this phenomenon. Reaction–diffusion equations (Lee et al., 2003; Qi et al., 2001) have been used to describe the spatiotemporal evolution of surface receptors and intracellular protein concentrations. These partial differential equations have been solved numerically both by finite difference (Qi et al., 2001) and finite element methods (Lee et al., 2003). A lattice model has also been used study the movement of the membrane proteins, in which proteins are represented by particles on a lattice (Lee et al., 2003) or on a set of membrane patches (Weikl and Lipowsky, 2004). The system evolution is solved by a kinetic Monte Carlo scheme which mimics the dynamics of receptor–ligand binding and protein movement. The majority of models focus on the study of the concentrations of key components and rates of events, rather than on the location and motion of individual molecules in a highly structured environment. Although some generic features of pattern formation and T-cell signalling are captured in these simplified models, relatively little is known concerning the spatial information associated with IS formation (Di Ventura et al., 2006) and the mechanisms by which receptor clustering is regulated.

Molecular dynamics (MD) simulations offer us the chance of viewing the unviewable, of measuring the unmeasurable, and of comprehending the seemingly incomprehensible. MD offers a dynamic, not a static view of molecular events. Previously, we have used supercomputing methods to undertake MD simulations of a variety of immunologically relevant molecular systems (Wan et al., 2005a,b). These studies have investigated the binding of the TCR with pMHCs by means of atomistic MD simulations. Recognition is not an isolated event: when pMHCs are recognized by TCR, many other co-receptors and accessory molecules are also involved. To simulate such larger systems on longer time scales, there is a need to adopt new algorithmic approaches in conjunction with novel computing paradigms. The increase in the size and timescale of simulations has been fuelled by the development of massively parallel MD codes which scale to hundreds of processors on high-end parallel platforms, by the speed of individual processors which is still doubling every 2 years or less, and by the advent of grid computing which achieves higher throughput computing by taking advantage of many networked computers. It is worth noting that the use of specialized hardware can make even longer and bigger simulations. It has already been reported that MD simulation on a Cell Broadband Engine, a specially designed processor able to compute non-bonded interactions efficiently, is over one order of magnitude faster than a single core standard processor (De Fabritiis, 2007).

A ternary model of the TCR–pMHC–CD4 complex based on X-ray crystallography reveals that TCR and CD4 co-localize to interact simultaneously with the same peptide-MHC class II (pMHCII) (Wang et al., 2001). The TCR binds to membrane-distal antigen peptide binding domains, while the CD4 co-receptor binds to the non-polymorphic surface of the membrane-proximal domains of the MHC molecule. An X-ray structure enables us to visualize protein structures at the atomic level and enhances our understanding of protein function. However, the crystallization can produce a particular conformational form which differs from those favoured within a physiological environment (Li et al., 2005). Atomistic simulations, while a considerable challenge from the perspective of methodology, would yield a rich dividend of understanding. Only dynamical simulations can capture the rich dynamic nature of the IS. Emergent behaviour characteristic of the IS would arise naturally from an MD simulation, rather than being imposed within macroscopic mathematical models.

Our study has, as its ultimate goal, a realistic molecular-based simulation of the IS. But we must build this up gradually and with rigour. Each step in the process must be validated and explored. That is the programme that we begin here. Fluorescence microscopy experiments have shown that a single agonist pMHC complex can trigger transient calcium signalling in the presence of CD4 (Irvine et al., 2002). Hence we start by looking at the smallest viable component of the IS, a model of the membrane-embedded complex comprising TCR–pMHC–CD4, focusing on the molecular details of the immunological synapse, which include pMHCII, TCR, CD4 co-receptor, and membrane (Fig. 1). We characterize the behaviour of our system thoroughly, compare it to experimental observations, and discuss the logistic feasibility of larger, longer simulations.

2. Methods

2.1. Software

The CHARMM (Brooks et al., 1983) and VMD (Humphrey et al., 1996) packages were used for preparing the initial molecular models and analyzing the simulation data. Modeller (Sali and Blundell, 1993) was used to build the transmembrane and extracellular loops missing in the X-ray structures. Explicit solvent molecular dynamics simulations were performed using NAMD (Kale et al., 1999).

2.2. Construction of the extracellular region of the complex

The TCR–pMHC–CD4 complex is composed of two crystal structures: the CD4 four domain molecule [PDB:1WIO] (Wu et al., 1997) and the TCR–pMHCII complex [PDB:1FYT] (Hennecke et al., 2000) (see Fig. 1). The TCR is a heterodimer of an α chain and a β chain. Each chain has a variable region and a constant region. The MHC class II molecule is also a heterodimer with α and β chains. The two chains form a groove at their membrane-distal end where the peptide binds. The CD4 is monomeric and has four extracellular IgSF domains D1–D4.

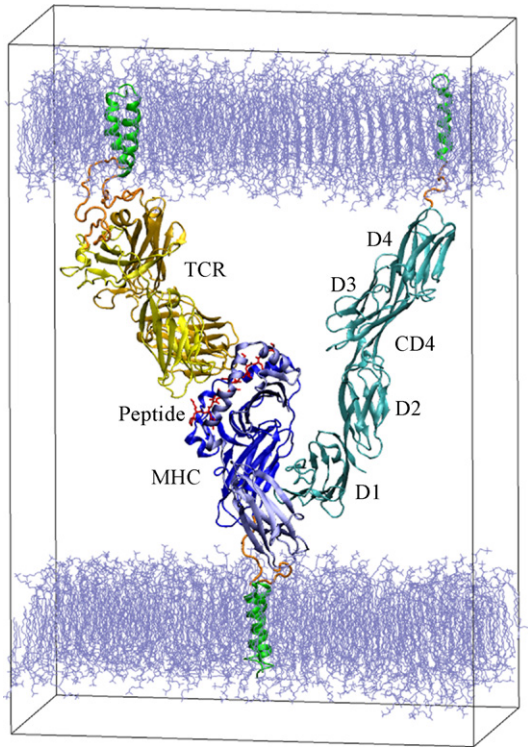

Fig. 1. The extracellular and transmembrane regions of the TCR–pMHC–CD4 complex with membrane in water box. The box is about 160 Å, 82 Å and 238 Å in its *x*, *y* and *z* dimensions, respectively. There are 329,265 atoms in the model. The stalk of MHCα chain is coloured in blue, MHCβ chain in light blue, peptide in red, TCRα chain in yellow, TCRβ chain in dark yellow and CD4 in cyan. The link regions are coloured in orange, transmembrane regions in green, and membrane in iceblue. The four domains of CD4 are indicated. Water molecules are not shown for clarity. The image was prepared using the programme VMD. (For interpretation of the references to colour in this figure legend, the reader is referred to the web version of the article.)

The D1–D2 and D3–D4 junctions of the CD4 molecule are quite rigid, with the D2–D3 junction itself having some flexibility. In the TCR–pMHCII X-ray structure, there are two loops missing, one in the β chain of MHCII and one in the α chain of TCR. The former was built from human class II MHC protein HLA-DR1 [PDB:1DLH] (Stern et al., 1994) and the latter from human A6-TCR [PDB:1QRN] (Ding et al., 1999), by overlapping the relative domains of 1FYT to those of 1DLH and 1QRN, respectively. The TCR–pMHCII and CD4 structures were incorporated together by superimposing the D1D2 domains of the four-domain CD4 and the binary pMHCII–D1D2 CD4 complex [PDB:1JL4] (Wang et al., 2001), and the pMHCII of the TCR–pMHCII and the binary pMHCII–D1D2 CD4. The TCR–pMHCII–CD4 ternary complex is of V-shape topology with the constant domains of pMHCII and the D1 of CD4 at the apex, the TCR–pMHCII and CD4 molecules being located at each ray. The complex was orientated so that the bisectrix of the V-shape complex was along the *z* axis and the V-shape in *xz* plane. The extracellular domains of the complex, which we refer to as 'stalks' hereafter, have stable secondary structures, their coordinates being taken from X-ray crystallography which is more reliable than those from homology modelling. The incorporation of the transmembrane and link regions is described next (note that neither the signal regions nor the cytoplastic tails were included). The link regions are the extracellular loops which connect the extracellular and transmembrane domains.

2.3. Construction of the link and transmembrane regions

The transmembrane and link regions of CD4, MHC and TCR were modelled using Modeller (Sali and Blundell, 1993). The residues modelled are listed in Table 1. The transmembrane and link regions are expected to be α-helices and coils, respectively. The orientation of these α-helices is set parallel to the *z* axis which is also the direction of the bisectrix of the V-shaped TCR–pMHC–CD4 complex and the membrane normal (see Fig. 1). To adjust the orientations of the α-helices, constrained MD simulations were performed to bring the transmembrane regions into the desired orientation. Only the link and transmembrane regions were allowed to move with restraints imposed to keep the transmembrane regions in α-helical geometries. Torques were applied on the α-helices to rotate them toward the *z* direction. The magnitudes of the torques applied were pro-

Table 1
Modelled residues in the link and transmembrane regions of MHC, TCR and CD4

Chain	Link	Transmembrane
MHCα	207–216 (181–190)	217–239 (191–213)
MHCβ	222–227 (191–196)	228–250 (197–219)
TCRα	222–250 (202–230)	251–270 (231–250)
TCRβ	262–282 (241–261)	283–304 (262–283)
CD4	389–396 (364–371)	397–418 (372–393)

The ranges are from the complete primary sequence as reported in the PDB SEQRES records, while the ranges used in the MD simulations are given in parentheses.

portional to the tangent of the angle between the longest axes of the α-helices and the z axis. This makes the rotations smooth when the directions of the axes are close to the z axis. After a series of constrained MD simulations, when the applied torques were small and did not decrease obviously, the α-helices were approximately parallel to the z axis.

2.4. Inclusion of membrane, counterions and water molecules

Two rectangular patches of bilayer were constructed in the xy plane, using the pre-built and solvated POPC lipids in VMD (Humphrey et al., 1996). The size of the patches was 20 Å larger in the x and y dimensions than those of the complex. The geometric centre of the complex was aligned with that of the lipid bilayers in the x and y dimensions. The membrane patches were moved along the z axis to embed the transmembrane regions of the complex within the membrane. Lipid molecules, along with the water molecules hydrating the lipid head groups, were removed if they overlapped with the protein. The complexes were rendered electrostatically neutral by adding counterions (Na^+) and then solvated using TIP3P water molecules (Jorgensen et al., 1983). The distance between the edges of the solvent box and the closest atom in the protein was 10 Å. This procedure resulted in a final atom count for the model of 329,265 (see Fig. 1).

2.5. Simulation

Atomic charges, van der Waals, and stereochemical force-field parameters were taken from the CHARMM22 proteins (MacKerell et al., 1998) and CHARMM27 lipids (Feller and MacKerell, 2000) all-atom force field. Periodic boundary conditions were applied in all three spatial dimensions. Particle Mesh Ewald (PME) (Toukmaji and Board, 1996) was used for the full electrostatic calculations. The van der Waals interactions were truncated using the switch method with a switch range of 10–12 Å. Hydrogen to heavy-atom bonds, and the internal geometry of the water molecules, were constrained using SHAKE (Ryckaert et al., 1977) and the equations of motion were integrated using a Verlet algorithm with a 2 fs timestep. Potential energy minimizations were firstly run with position restraints on heavy protein atoms to remove any specious high-energy contacts. Then a series of simulations were performed with the backbone atoms, and initially also the heavy atoms of protein side-chains and the membrane, harmonically restrained at their initial positions. This was followed by free dynamics, assigning random velocities based on a Maxwellian distribution at 100 K as the initial temperature. The systems were heated to the final temperature of 300 K by periodically reassigning the velocities. A weak-coupling algorithm (Berendsen et al., 1984) was applied to maintain the system at 300 K and 1 atm pressure. The production runs were 10 ns long, for which the NAMD (Kale et al., 1999) package was used, running on 128 processors of the SGI Altix at CSAR (University of Manchester, UK). The time needed to simulate a nanosecond of molecular dynamics on such a system was about 23.00 h.

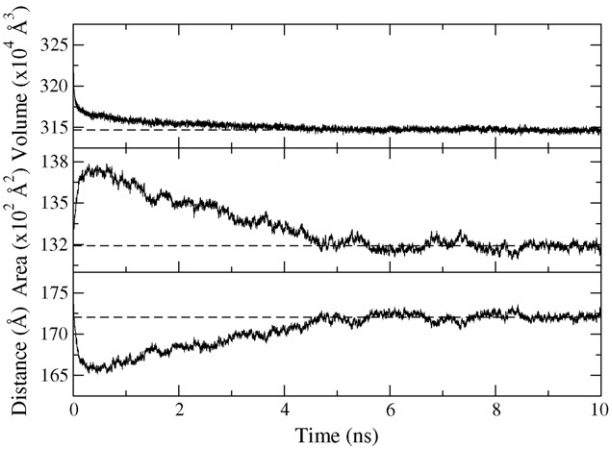

Fig. 2. Time evolutions of the volume, membrane surface area and distance between two membranes. All three properties converge to stable values after 5 ns.

3. Results

3.1. System equilibrium

To assess when the entire system is equilibrated, we analysed the time-dependences of the surface area of membrane, the intermembrane distance and the volume of the entire system (Fig. 2). The membrane surface area increases quickly in the first 0.3 ns because of the strong repulsive interactions among the lipid molecules, and between the lipid and the transmembrane regions of the proteins, followed by a smooth decrease until 5 ns because of the conformational adjustment of the lipid and proteins. The distance between the two membranes was measured as that between the centres of the bilayers on the z axis, which has converse behaviour to the surface area of membrane. The initial steep decrease of the distance is due to the increase of the membrane area, as well as the adjustment of the water box to reasonable density. The distance then increases smoothly as a result of the decrease of membrane area. The volume of the box exhibits a steep decrease from the initial packing until 0.3 ns, then a smooth decrease up to 5 ns. The volume, the membrane surface area and the distance between the two lipid bilayers all converge to stable values after 5 ns. The distance is around 172.1 Å after 5 ns simulation. Taking into account the thickness of the POPC bilayer (∼40 Å), the intermembrane distance is comparable with the dimensions of accessory molecule CD2/CD48 (∼140 Å) which enhances T-cell antigen recognition, and smaller than elongated CD48 (>210 Å) which inhibits recognition (Wild et al., 1999). This value is also in the range (120–150 Å) measured experimentally in the contact area between cytotoxic T cells and target cells (Biberfeld and Johansson, 1975). Some limited flexibility in intermembrane distance is necessary as it is unlikely that all molecules involved in T-cell antigen recognition will span exactly the same distance. Some tilting of these molecules relative to the plane of the membranes, as shown for all three proteins in this model (Fig. 1), can adjust the distance of adjacent bilayers to regulate a close-contact zone.

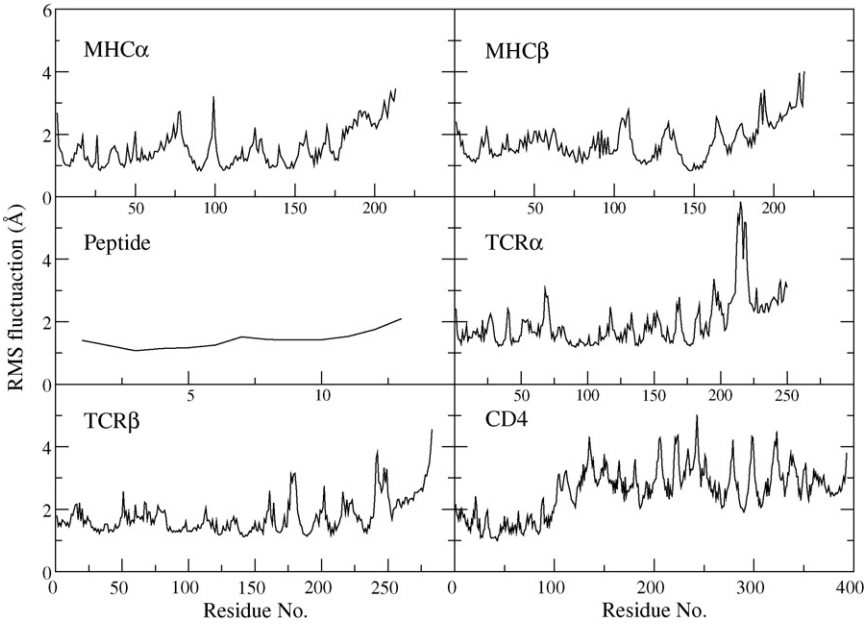

Fig. 3. Residue-by-residue RMS fluctuations of each chain. Most residues in stalks of MHC and TCR, and in peptide have less than 2 Å fluctuations. The large fluctuations in the D2–D4 domains of CD4 come from the inter-domain motions relative to the stalk of TCRpMHC and the D1 domain.

3.2. The root-mean-square (RMS) fluctuations of the complex

The RMS fluctuations were calculated using the last 5 ns trajectory where the entire system remains at equilibrium (see Fig. 2). The average structure of the TCR–pMHC–CD4 complex over the last 5 ns was used as the reference. The fluctuation of each residue from the average structure was calculated after least squares alignment of each frame with the average structure. Note that the conformation was fitted better at the TCR–pMHC stalk than the CD4 stalk because of the higher atomic density within the TCR–pMHC region. Both TCR and MHC have reasonable fluctuations in the last 5 ns trajectories (Fig. 3), apart from the link and transmembrane regions which may need a longer time to equilibrate, or may have multiple conformations. The secondary structures of TCR and MHC, as well as the peptide, are very stable and have small fluctuations. The TCRα link region is the longest coil (29 amino acids) among all modelled regions and is the most flexible part. The CD4 comprises four immunoglobulin-like domains D1–D4. The D1 domain (residues 1–98) has small fluctuations, while the D2–D4 domains have relatively large fluctuations because of the inter-domain motions of these domains relative to TCRpMHC and the D1 domain. When the RMS fluctuation was calculated by alignment of each domain with its own average structure, the RMS values were smaller, especially for the D2–D4 domains of CD4 (2.1 Å smaller on average for each residue), compared with those obtained by alignment of the entire complex. The relatively small overall RMS fluctuations for the entire complex and small intra-domain fluctuations indicate that the stalks of the various proteins are stable, giving us confidence in the use of these simulations for further analysis of the interactions of the proteins in the bilayer environment.

3.3. Protein–membrane and protein–protein interactions

To quantify the protein–membrane and protein–protein interactions, we calculate the numbers of contacts which are measured as a function of time. A contact is assumed to exist when a protein–lipid or protein–protein interatomic distance is less than 3.5 Å. The numbers of contacts between proteins (pMHC, TCR and CD4) and lipid are roughly constant over the duration of the simulation, including the first 5 ns equilibrium period (Fig. 4a). The constant number of contacts implies reasonable quality of the homology modelling for the transmembrane regions of the proteins, and reasonable integration of the regions into membrane. For the number of contacts between CD4 and membrane, there is a smooth increase in the first half of the 10 ns simulation, followed by a decrease in the second half. The variation reflects the slow conformational adjustments of the transmembrane region of CD4.

The number of contacts between pMHC and TCR decreases during the first 3 ns simulation; the decrease of the intermembrane distance at the beginning of the simulation does not lead to compression at the TCR–pMHC interface (see Fig. 4b). The number of contacts between pMHC and CD4 is about 142 in the first 3.5 ns simulation, increasing up to ∼216 in the next 1.5 ns, subsequently remaining sensibly constant around this value.

3.4. Variation of the V-shape of the complex

To examine the overall shape of the TCRpMHC–CD4 complex, the relative orientation of the stalks of TCRpMHC and CD4 was measured. The orientation of TCRpMHC was defined as the direction of the vector spanning from the geometric centre of the pMHC to the geometric centre of the TCR, while the orientation of CD4 was from the geometric centre of D1–D2 to the

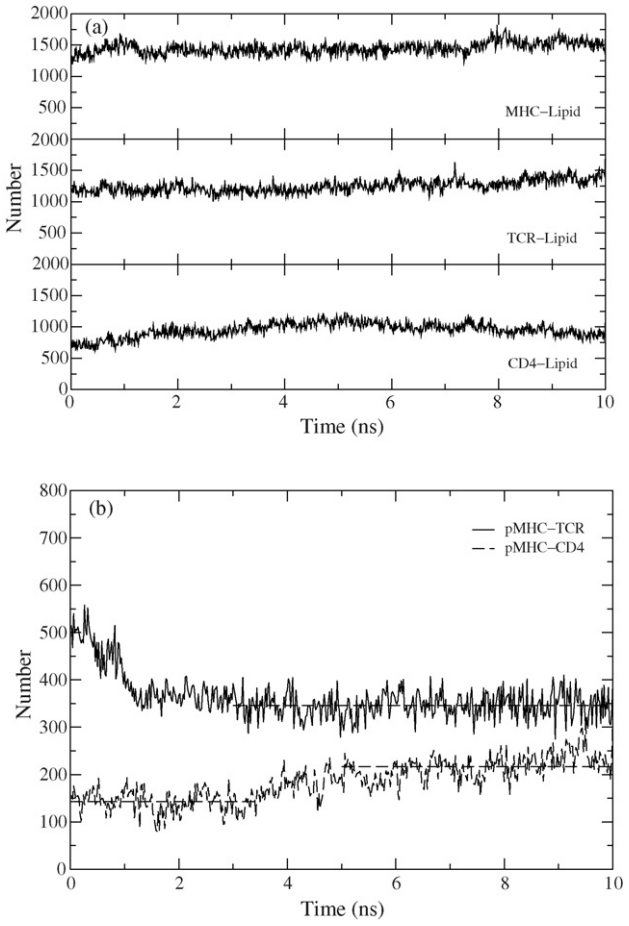

Fig. 4. The number of close contacts as a function of time. The number of close contacts for (a) protein–lipid and (b) protein–protein. The numbers of contacts between proteins and lipid are roughly constant over the 10 ns simulation. The number of contacts between pMHC and TCR reaches a plateau after ∼3 ns; that between pMHC and CD4 is about 142 in the first 3.5 ns simulation, and ∼216 in the last 5 ns.

geometric centre of D3–D4 domains. The angles between these two vectors (TCRpMHC–CD4), and each vector with the z axis (TCRpMHC–z and CD4–z) are shown in Fig. 5. All angles are stable during the simulation, with apparently long-time scale fluctuations of ∼10 ns (our simulation is not long enough to confirm this definitively). The angle between the two vectors is approximately equal to the sum of the angles each vector makes with the z axis along the whole 10 ns trajectory.

The two vectors are usually skew lines which do not intersect and are not in the same plane. The minimum distance between these two vectors was calculated to further examine the overall shape of the complex (Fig. 5). The distance was defined as the length of the transversal perpendicular to both vectors. The distances of each vector from the z axis were also likewise measured. The distance between TCRpMHC and the z axis is stable, with small accompanying fluctuations, while that between CD4 and the z axis fluctuates more substantially. The flexibility between D2 and D3 domains of CD4 effectively makes its four domains into two relative rigid segments. The angle between the longest axes of these two fragments fluctuates significantly during the simulation, between 120.8° and 150.6°. The large fluctuations in the CD4–z axis distance indicate the inter-domain movement of the CD4 molecule. This observation agrees well with electron microscopy studies of CD4 which suggest a considerable degree of segmental flexibility (Davis et al., 2003).

3.5. Thermodynamic properties

To obtain approximate thermodynamic predictions, we have carried out molecular mechanics Poisson–Boltzmann surface area (MM/PBSA) (Wan et al., 2005b) calculations to estimate the binding free energies of TCR–pMHC and pMHC–CD4. The last 5 ns trajectory was used. The snapshots of the unbound proteins were extracted from the single trajectory of the complex. MM/PBSA approximates free energies using molecular

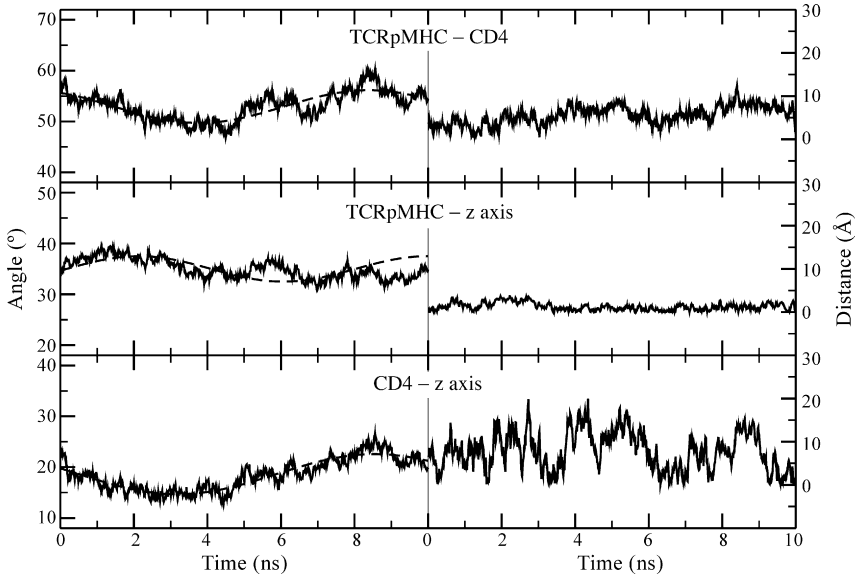

Fig. 5. Angles and distances of the V-shaped complex. Angles and distances between vectors of TCRpMHC and CD4, the vector of TCRpMHC and the z axis, the vector of CD4 and the z axis. The angles and distances are roughly constant, except for the distance between CD4 and the z axis. The apparently long-time scale fluctuations for the angles are indicated by dash lines.

mechanics energies and a Poisson–Boltzmann continuum representation of the solvent, together with a surface-dependent term using snapshots from MD simulations generated with explicit solvent. Attempts have been made to evaluate all formally relevant MM/PBSA terms for the Ras–Raf complex (Gohlke and Case, 2004), which clearly illustrate the magnitude of the convergence problems for entropy estimation. The convergence problem is much more severe for very large systems such as the present one. Due to insufficient phase space sampling over the duration of last 5 ns trajectory, and no simulations being done for unbound TCR–pMHC and pMHC/CD4 proteins, it is not possible to calculate the conformational entropy upon binding. Therefore, entropic calculations were not performed. The energetic parts were calculated every 20 ps, with uncertainties estimated by a block average method (Wan et al., 2004) using 10 blocks. The calculated energies were compared with the enthalpies from experiment where available.

The MM/PBSA energetic result is -46.9 ± 2.9 kcal/mol for the TCR–pMHC interaction, which is in fair agreement with the enthalpies, usually ranging from -10 to -30 kcal/mol, measured by van't Hoff analysis or calorimetric experiments (Krogsgaard and Davis, 2005). The calculated binding enthalpy is -26.9 ± 2.5 kcal/mol for the CD4–pMHC interaction; there is no experimental enthalpy available to compare with the binding of CD4 to pMHC. Although entropic calculations are not possible from our simulations, some experimental information has been obtained for the entropy changes of TCR–pMHC binding. In most cases, there is a highly unfavourable entropic effect associated with TCR–pMHC binding, indicative of substantial conformational adjustments and reduction in conformational flexibilities upon binding (Krogsgaard and Davis, 2005). An induced fit model has been suggested for such protein–ligand associations, in which local folding is coupled to binding (Boniface et al., 1999). The CD4–pMHC binding, however, is categorized as a "rigid-body" association (Gao et al., 2002). The entropy is not expected to make a large contribution to the CD4–pMHC binding free energy. The affinity of an interaction is defined as its binding free energy ΔG, a sum of enthalpic (ΔH) and entropic ($-T\Delta S$) components. The ΔGs are ~ -7 kcal/mol for TCR–pMHC, and > -5 kcal/mol for CD4–pMHC (Davis et al., 2003) in a bulk (3D) environment.

In order for specialized cells to interact with each other, TCRs, MHCs and their co-factors must function on the cell surface. Such surfaces are formed from lipid bilayers, which are a quasi two-dimensional (2D) environment. Measuring such 2D thermodynamic properties is technically difficult. A few 2D experiments have been done for the T-cell surface molecules CD2 and CD28, in which molecules were tethered on glass-supported planar lipid bilayers (Dustin et al., 2001). It has been argued that there is a nonlinear relationship between 3D and 2D binding affinities (Davis et al., 2003). In our simulation, the molecules are all effectively tethered to membranes; hence the estimated energy represents a 2D calculation. Unfortunately, there are no equivalent experimental 2D values available to compare with our calculations. The experimental 3D enthalpies are thought to be similar to the values they would have in 2D (Dustin et al., 2001) although this could be debated. Exact comparison of the binding free energies is not possible here both because of the lack of an entropy calculation in our simulations and owing to the simulations being performed on proteins bound to two bilayers.

Because of the limitations of the computational method and the difficulties of making relevant experimental measurements, the comparison of the thermodynamic properties we are able to make here is partial and thus incomplete. However, the purpose of the simulations, at this stage, is to gain mechanistic insight, rather than to produce quantitatively accurate thermodynamic results for the IS. With further information on the protein–protein and protein–membrane interactions, extrapolation can be made to more and more realistic IS models using atomistic- or molecular-based simulations (see Section 4). Additional insight will be gained from these simulations, which is difficult, if not impossible, to obtain from experiments.

4. Discussion

Over the past decade, structural and thermodynamic details of the key protein interactions involved in the T-cell recognition event have been revealed (van der Merwe and Davis, 2003). The interplay among these molecules results in IS formation and the ensuing signalling processes, which have been observed using different experimental methods (Huppa and Davis, 2003) and studied using simplified models (Lee et al., 2003; Qi et al., 2001). However, the structural dimension is omitted, either explicitly or implicitly, from much of such experimental and computational biology: the behaviour of proteins is inferred indirectly rather than being studied directly. The dynamic behaviour of biological systems at the molecular level is also largely excluded. In this study, we have used molecular dynamics simulations to study the atomistic details of receptor–ligand recognition at a cell–cell junction. A quantitative model was constructed for T-cell recognition by modelling the TCR–pMHC–CD4 complex, embedded in two opposed membranes. The structural stability of the complex was examined carefully and compared with experiments where possible. Thermodynamic properties were estimated by the MM/PBSA method and compared with experimental data; although quantitative comparisons are not possible, qualitative agreement is obtained and many insights gained.

Many molecules are involved in the formation of an IS, both in terms of the types of molecules and also in terms of their number. The resulting system is complex and serves as an archetype of the spatio-temporal organisation in three-dimensions implicit in biology and as a prototype for the methods, both experimental and computational, needed to understand such systems. The IS is composed of soluble proteins (such as those involved in the cytoskeleton, as well as signalling molecules) and membrane proteins, which are embedded into two complex lipid bilayers, as well as a large population of intracellular and extracellular solvent molecules. These components combine to create a complex system which challenges current methodology both computational and experimental.

The binding of one pair of proteins affects the propensity of other pairs to bind by bringing the lipid bilayers from APC and T cell into proximity, and by changes in the lateral mobility

of receptors and their ligands. We are now taking the next step by simulating an extended model, in which four sets of TCR–pMHC–CD4 complexes are included. This fully atomistic model, including explicit water and lipid molecules, is approximately one million atoms in size. A simulation for a similar size system has recently been published (Freddolino et al., 2006). It takes less than 1 day to simulate a nanosecond of such a system on 256 processors of a large multi-processor machine, while an efficient solution (in terms of elapsed wall clock time) on the Grid is also available through the distribution of many simulations over a set of supercomputers (Coveney, 2005).

There are hundreds of different molecules involved in IS formation and signalling processes, which would require tens of millions atoms for proteins in an atomistic molecular model. The models would be one order of magnitude larger if all water and deformable lipid molecules were explicitly included. Such a system will not be tractable using standard molecular dynamics simulation for many years, especially on long time scales. The recently developed hybrid atomistic/coarse-grained molecular dynamics simulations (Diestler et al., 2006) may enable progress to be made: the binding domains can be simulated using atomistic models and others using a coarse-grained (CG) model, with mesoscopic representations of water and lipid. The domain description for proteins (Qi et al., 2006) could be used for the atomistic/coarse-grained definitions. The number of atoms and coarse-grained particles would thereby be decreased to a few millions, which would lie within the capacity of MD simulation (Sanbonmatsu and Tung, 2007).

From a biological perspective, many questions remain concerning the formation of the IS. One is the role of lipid rafts. Several authors have explored this issue with simulations. Nicolau et al. (2006), using an empirical approach, showed that the segregation of moving proteins is largely independent of the size, viscosity, and mobility of rafts. More recently, Nicolau et al. (2007) undertook stochastic random walk modelling of protein diffusion in a cell membrane, where three interactions were analysed: collisions with mobile and static obstacles, and capture by or exclusion from lipid rafts. Their results indicated that the preferential partitioning of proteins into rafts had little effect on apparent diffusion whereas exclusion had a significant effect on diffusion. The influence of lipid rafts on IS formation could be analysed by integrating MD results with the outcome of calculations such as this. Another unanswered question concerns the role of the cytoskeleton. Zhu et al. (2007) have investigated membrane/cytoskeleton dynamics by coupling the actin–spectrin network (modelled as a combined Brownian dynamics model of the actin protofilament and a modified cable-dynamics wormlike-chain model of spectrin) to a Fourier space Brownian dynamics model of the lipid bilayer. Their work indicates the importance of a three-dimensional analysis and the effect of protein–lipid coupling on the dynamic behaviour of cell membrane. The prospect of a synergistic combination of their broad-brush approach and our detailed atomistic approach is tantalising and compelling.

However, the timescale for IS formation and maturation (about 30 min) is still out of reach as it is determined by the timestep intrinsic to atomistic simulations. By contrast, pure coarse-grained descriptions of large-scale phenomena can reach a wide spectrum of length and time scales (Baschnagel et al., 2000). Common CG simulations use the one-to-one correspondence of a 'bead' to a specific group of atoms. An even coarser grained description can be used to simulate IS formation in which each protein or each domain of a protein is coarse-grained into a soft ellipsoidal particle. In such a purely mesoscopic model, the number of particles will be dramatically reduced and the timestep substantially increased ($\sim 10^9$ times greater than atomistic MD), which should make simulations of IS formation over many time and length scales possible. The outstanding challenge is to reliably connect the atomistic level to the hybrid atomistic/coarse-grained level, then to the even coarser level at which full IS formation can be modelled.

5. Conclusions

The study outlined in this paper is the first step in a long journey leading to a full model of the immune synapse. At least "schematically", the route that journey will take is clear. Additional pMHC–TCR units would be added to the simulation. Larger and larger areas of opposed membrane would be simulated. Other components of the IS, such as complexes between leukocyte function-associated antigen 1 (LFA-1) and intercellular adhesion molecule 1 (ICAM-1) would be added. The segregation into concentric rings could then be simulated and observed directly. As a complete view of the formation of the IS is beyond the scope of current experimental methods, multi-scale MD simulations may be the best opportunity we have to reach a full understanding of this remarkable supra-macromolecular event.

In physics, and increasingly in chemistry, theory and computation stand shoulder-to-shoulder with experiment. Computational simulation is seen as an appropriate and a valid means of improving our understanding of the world around us; not the local macroscopic world of our every-day experience but the invisible worlds of the very small and the very large which impact us as significantly as the things we see and touch and taste and smell. We have long known that there is nothing in biology which is fundamentally inconsistent or incommensurable with mathematics, chemistry, and physics. Biology long ago rejected vitalism. The only information needed for life is provided by an organism's chemical constituents. It is unlikely in the extreme that living systems cannot be understood in terms of chemistry and physics. So-called emergent properties are a straightforward manifestation of changing scales within systems and there is little need to reject reductionism on their behalf. Yet we need to build from reductionism, embracing the holistic integration of science at many scales. This is something only computation can do, weaving together disparate experimental and theoretical results using the techniques of simulation. The day is coming when theory and computation will guide biology, as it does physics now. Experiment will exist to verify prediction rather than theory existing to rationalise and explain experiment. Immunology in general, and the immune synapse in particular, provides a perfect target for such endeavours, com-

bining as it does utilitarian importance with a need to explore its characteristics at various length scales. It is only through the integration of diverse experimental and computational results that we can achieve a cohesive understanding of immunological defence against disease.

Acknowledgements

The authors and the Jenner Institute (formally, The Edward Jenner Institute for Vaccine Research) wish to thank its erstwhile sponsors GlaxoSmithKline, the Medical Research Council (MRC), the Biotechnology and Biological Sciences Research Council (BBSRC), and the UK Department of Health. We thank the Engineering and Physical Sciences Research Council (EPSRC) for funding this research through RealityGrid Grant GR/R67699 and associated Platform Grant EP/C536452, which provided access to the Computer Services for Academic Research (CSAR). PVC and SW are also grateful to BBSRC for support via IntBioSim Grant BBS/B/16011.

References

Baschnagel, J., Binder, K., Doruker, P., Gusev, A.A., Hahn, O., Kremer, K., Mattice, W.L., Muller-Plathe, F., Murat, M., Paul, W., Santos, S., Suter, U.W., Tries, V., 2000. Bridging the gap between atomistic and coarse-grained models of polymers: status and perspectives. Advances in polymer science: viscoelasticity, atomistic models. Stat. Chem. 152, 41–156.

Berendsen, H.J.C., Postma, J.P.M., Vangunsteren, W.F., Dinola, A., Haak, J.R., 1984. Molecular-dynamics with coupling to an external bath. J. Chem. Phys. 81, 3684–3690.

Biberfeld, P., Johansson, A., 1975. Contact areas of cytotoxic lymphocytes and target-cells—electron-microscopic study. Exp. Cell Res. 94, 79–87.

Boniface, J.J., Reich, Z., Lyons, D.S., Davis, M.M., 1999. Thermodynamics of T-cell receptor binding to peptide-MHC: evidence for a general mechanism of molecular scanning. Proc. Natl. Acad. Sci. U.S.A. 96, 11446–11451.

Bromley, S.K., Burack, W.R., Johnson, K.G., Somersalo, K., Sims, T.N., Sumen, C., Davis, M.M., Shaw, A.S., Allen, P.M., Dustin, M.L., 2001. The immunological synapse. Annu. Rev. Immunol. 19, 375–396.

Brooks, B.R., Bruccoleri, R.E., Olafson, B.D., States, D.J., Swaminathan, S., Karplus, M., 1983. Charmm—A program for macromolecular energy, minimization, and dynamics calculations. J. Comput. Chem. 4, 187–217.

Coveney, P.V., 2005. Scientific grid computing. Phil. Trans. R. Soc. A: Math. Phys. Eng. Sci. 363, 1707–1713.

Davis, S.J., Ikemizu, S., Evans, E.J., Fugger, L., Bakker, T.R., van der Merwe, P.A., 2003. The nature of molecular recognition by T cells. Nat. Immunol. 4, 217–224.

De Fabritiis, G., 2007. Performance of the cell processor for biomolecular simulations. Comput. Phys. Commun. 176, 660–664.

Di Ventura, B., Lemerle, C., Michalodimitrakis, K., Serrano, L., 2006. From in vivo to in silico biology and back. Nature 443, 527–533.

Diestler, D.J., Zhou, H., Feng, R., Zeng, X.C., 2006. Hybrid atomistic-coarse-grained treatment of multiscale processes in heterogeneous materials: a self-consistent-field approach. J. Chem. Phys. 125, 064705.

Ding, Y.H., Baker, B.M., Garboczi, D.N., Biddison, W.E., Wiley, D.C., 1999. Four A6-TCR/peptide/HLA-A2 structures that generate very different T-cell signals are nearly identical. Immunity 11, 45–56.

Dustin, M.L., Bromley, S.K., Davis, M.M., Zhu, C., 2001. Identification of self through two-dimensional chemistry and synapses. Annu. Rev. Cell Dev. Biol. 17, 133–157.

Dustin, M.L., Tseng, S.Y., Varma, R., Campi, G., 2006. T cell-dendritic cell immunological synapses. Curr. Opin. Immunol. 18, 512–516.

Feller, S.E., MacKerell, A.D., 2000. An improved empirical potential energy function for molecular simulations of phospholipids. J. Phys. Chem. B 104, 7510–7515.

Freddolino, P.L., Arkhipov, A.S., Larson, S.B., McPherson, A., Schulten, K., 2006. Molecular dynamics simulations of the complete satellite tobacco mosaic virus. Structure 14, 437–449.

Gao, G.F., Rao, Z.H., Bell, J.I., 2002. Molecular coordination of alpha beta T-cell receptors and coreceptors CD8 and CD4 in their recognition of peptide-MHC ligands. Trends Immunol. 23, 408–413.

Gohlke, H., Case, D.A., 2004. Converging free energy estimates: MM–PB(GB)SA studies on the protein–protein complex Ras–Raf. J. Comput. Chem. 25, 238–250.

Grakoui, A., Bromley, S.K., Sumen, C., Davis, M.M., Shaw, A.S., Allen, P.M., Dustin, M.L., 1999. The immunological synapse: a molecular machine controlling T-cell activation. Science 285, 221–227.

Hennecke, J., Carfi, A., Wiley, D.C., 2000. Structure of a covalently stabilized complex of a human alpha beta T-cell receptor, influenza HA peptide and MHC class II molecule. HLA-DR1. EMBO J. 19, 5611–5624.

Humphrey, W., Dalke, A., Schulten, K., 1996. VMD: visual molecular dynamics. J. Mol. Graph. 14, 33–38.

Huppa, J.B., Davis, M.M., 2003. T-cell-antigen recognition and the immunological synapse. Nat. Rev. Immunol. 3, 973–983.

Irvine, D.J., Purbhoo, M.A., Krogsgaard, M., Davis, M.M., 2002. Direct observation of ligand recognition by T cells. Nature 419, 845–849.

Jorgensen, W.L., Chandrasekhar, J., Madura, J.D., Impey, R.W., Klein, M.L., 1983. Comparison of simple potential functions for simulating liquid water. J. Chem. Phys. 79, 926–935.

Kale, L., Skeel, R., Bhandarkar, M., Brunner, R., Gursoy, A., Krawetz, N., Phillips, J., Shinozaki, A., Varadarajan, K., Schulten, K., 1999. NAMD2: greater scalability for parallel molecular dynamics. J. Comput. Phys. 151, 283–312.

Krogsgaard, M., Davis, M.M., 2005. How T cells 'see' antigen. Nat. Immunol. 6, 239–245.

Lee, K.H., Dinner, A.R., Tu, C., Campi, G., Raychaudhuri, S., Varma, R., Sims, T.N., Burack, W.R., Wu, H., Kanagawa, O., Markiewicz, M., Allen, P.M., Dustin, M.L., Chakraborty, A.K., Shaw, A.S., 2003. The immunological synapse balances T-cell receptor signaling and degradation. Science 302, 1218–1222.

Li, J., Correia, J.J., Wang, L., Trent, J.O., Chaires, J.B., 2005. Not so crystal clear: the structure of the human telomere G-quadruplex in solution differs from that present in a crystal. Nucleic Acids Res. 33, 4649–4659.

MacKerell, A.D., Bashford, D., Bellott, M., Dunbrack, R.L., Evanseck, J.D., Field, M.J., Fischer, S., Gao, J., Guo, H., Ha, S., Joseph-McCarthy, D., Kuchnir, L., Kuczera, K., Lau, F.T.K., Mattos, C., Michnick, S., Ngo, T., Nguyen, D.T., Prodhom, B., Reiher, W.E., Roux, B., Schlenkrich, M., Smith, J.C., Stote, R., Straub, J., Watanabe, M., Wiorkiewicz-Kuczera, J., Yin, D., Karplus, M., 1998. All-atom empirical potential for molecular modeling and dynamics studies of proteins. J. Phys. Chem. B 102, 3586–3616.

Nicolau, D.V., Burrage, K., Parton, R.G., Hancock, J.F., 2006. Identifying optimal lipid raft characteristics required to promote nanoscale protein–protein interactions on the plasma membrane. Mol. Cell. Biol. 26, 313–323.

Nicolau, D.V., Hancock, J.F., Burrage, K., 2007. Sources of anomalous diffusion on cell membranes: a Monte Carlo study. Biophys. J. 92, 1975–1987.

Qi, S.Y., Groves, J.T., Chakraborty, A.K., 2001. Synaptic pattern formation during cellular recognition. Proc. Natl. Acad. Sci. U.S.A. 98, 6548–6553.

Qi, S.Y., Krogsgaard, M., Davis, M.M., Chakraborty, A.K., 2006. Molecular flexibility can influence the stimulatory ability of receptor–ligand interactions at cell–cell junctions. Proc. Natl. Acad. Sci. U.S.A. 103, 4416–4421.

Ryckaert, J.P., Ciccotti, G., Berendsen, H.J.C., 1977. Numerical-integration of cartesian equations of motion of a system with constraints—molecular-dynamics of *n*-alkanes. J. Comput. Phys. 23, 327–341.

Sali, A., Blundell, T.L., 1993. Comparative protein modeling by satisfaction of spatial restraints. J. Mol. Biol. 234, 779–815.

Sanbonmatsu, K.Y., Tung, C.S., 2007. High performance computing in biology: multimillion atom simulations of nanoscale systems. J. Struct. Biol. 157, 470–480.

Stern, L.J., Brown, J.H., Jardetzky, T.S., Gorga, J.C., Urban, R.G., Strominger, J.L., Wiley, D.C., 1994. Crystal-structure of the human class-Ii MHC protein Hla-Dr1 complexed with an influenza-virus peptide. Nature 368, 215–221.

Toukmaji, A.Y., Board, J.A., 1996. Ewald summation techniques in perspective: a survey. Comput. Phys. Commun. 95, 73–92.

van der Merwe, P.A., Davis, S.J., 2003. Molecular interactions mediating T-cell antigen recognition. Annu. Rev. Immunol. 21, 659–684.

Wan, S.Z., Stote, R.H., Karplus, M., 2004. Calculation of the aqueous solvation energy and entropy, as well as free energy, of simple polar solutes. J. Chem. Phys. 121, 9539–9548.

Wan, S.Z., Coveney, P.V., Flower, D.R., 2005a. Molecular basis of peptide recognition by the TCR: affinity differences calculated using large scale computing. J. Immunol. 175, 1715–1723.

Wan, S.Z., Coveney, P.V., Flower, D.R., 2005b. Peptide recognition by the T-cell receptor: comparison of binding free energies from thermodynamic integration, Poisson–Boltzmann and linear interaction energy approximations. Phil. Trans. R. Soc. A-Math. Phys. Eng. Sci. 363, 2037–2053.

Wang, J.H., Eck, M.J., 2003. Assembling atomic resolution views of the immunological synapse. Curr. Opin. Immunol. 15, 286–293.

Wang, J.H., Meijers, R., Xiong, Y., Liu, J.H., Sakihama, T., Zhang, R.G., Joachimiak, A., Reinherz, E.L., 2001. Crystal structure of the human CD4 N-terminal two-domain fragment complexed to a class II MHC molecule. Proc. Natl. Acad. Sci. U.S.A. 98, 10799–10804.

Weikl, T.R., Lipowsky, R., 2004. Pattern formation during T-cell adhesion. Biophys. J. 87, 3665–3678.

Wild, M.K., Cambiaggi, A., Brown, M.H., Davies, E.A., Ohno, H., Saito, T., van der Merwe, P.A., 1999. Dependence of T-cell antigen recognition on the dimensions of an accessory receptor–ligand complex. J. Exp. Med. 190, 31–41.

Wu, H., Kwong, P.D., Hendrickson, W.A., 1997. Dimeric association and segmental variability in the structure of human CD4. Nature 387, 527–530.

Zhu, Q., Vera, C., Asaro, R.J., Sche, P., Sung, L.A., 2007. A hybrid model for erythrocyte membrane: a single unit of protein network coupled with lipid bilayer. Biophys. J. 93, 386–400.